Chemical Geology 158 (1999) 173–188

CHEMICAL GEOLOGY
INCLUDING
ISOTOPE GEOSCIENCE

sediments: evidence from the strontium isotope systematic

A. Eisenhauer [a,d,*], H. Meyer [a,b], V. Rachold [b], T. Tütken [a], B. Wiegand [a,c], B.T. Hansen [c], R.F. Spielhagen [d], F. Lindemann [d], H. Kassens [d]

[a] *Geochemisches Institut, Goldschmidtstr. 1, 37077 Göttingen, Germany*
[b] *Alfred-Wegener Institut für Polar- und Meeresforschung, Telegrafenberg A43, 14473 Potsdam, Germany*
[c] *Institut für Geologie und Dynamik der Lithosphäre, Goldschmidtstr. 3, 37077 Göttingen, Germany*
[d] *GEOMAR, Forschungszentrum für Marine Geowissenschaften, Wischofstr. 1-3, 24148 Kiel, Germany*

Received 20 August 1998; accepted 27 January 1999

Abstract

The $^{87}Rb/^{86}Sr$ and $^{87}Sr/^{86}Sr$ ratios of Laptev Sea sediments, of Arctic Ocean sediments and of suspended particulate matter (SPM) from Siberian rivers (Lena and Khatanga) form ‘pseudo-isochrons’ due to grain-size separation processes which are referred to as ‘Lena Mixing Envelope’ (LME) and as ‘Flood Basalt Envelope’ (FBE). At the land–ocean transition the reduction of the particle velocity causes a deposition of coarser grained material and the contact with saline water enhances a precipitation of finer-grained material. The coarse-grained material is enriched in Sr showing less radiogenic $^{87}Sr/^{86}Sr$ ratios whereas fine grained material is depleted in Sr relative to Rb showing more radiogenic $^{87}Sr/^{86}Sr$ ratios. The experimentally determined spread of the $^{87}Rb/^{86}Sr$ and $^{87}Sr/^{86}Sr$ ratios as a function of grain size in one sediment sample is on the same order as the natural spread of the $^{87}Sr/^{86}Sr$ ratios observed in all samples from the Arctic Ocean. Chemical Index of Alteration (CIA) for the Lena river SPM tend to confirm previous observations that chemical alteration is negligible in the Arctic environment. Thus, these ‘pseudo-isochrons’ reflect an average age and the average isotope composition in the river drainage area. Calculated apparent ages from the FBE reflect the age of the Siberian flood basalt of about 220 Ma and the initial ratio of 0.707(1) reflects their mantle origin. The age calculated from the LME of about 125 Ma reflects accidentally the Jurassic and Cretaceous age of the sediments drained by the Lena river and the initial ratio of 0.714(1) reflects the crustal origin of their source rocks. Comparison of geographical locations reveals that all samples from the eastern Laptev Sea (east of 120°E) fall along the LME whereas all samples from the western Laptev Sea (west of 120°E) fall between LME and FBE. Mixing calculations based on $^{143}Nd/^{144}Nd$ measurements, not influenced by grain size, show that about 75% of the western Laptev Sea sediments originate from the Lena drainage area whereas about 25% of the sediments are delivered from the Siberian flood basalt province. Sediments from the central Arctic Ocean are isotopically related to the Lena drainage area and the Siberian flood basalt province. However, sediments from the Arctic

* Corresponding author. Geochemisches Institut, Goldschmidtstr. 1, 37077 Göttingen, Germany. Tel.: +49-551-392216; fax: +49-551-393982; e-mail: aeisenh@gwgd.de

PII: S0009-2541(99)00026-1

Ocean margins close to Novaya Semlya, Greenland, the Fram Strait and Svalbard originate from sources not yet identified.

Keywords: Arctic Ocean; East-Siberia; $^{87}Sr/^{86}Sr$; $^{143}Nd/^{144}Nd$; Sediments; Rivers

1. Introduction

One important objective of modern geological and geochemical studies in the Arctic environment focuses on the understanding of the present and past activity of the large Siberian rivers Khatanga, Lena, Ob, Yana and Yenisei (Huh and Edmond, 1996; Hölemann et al., 1996; Kassens et al., 1996). Understanding the activity of these rivers is desirable because sea ice formation is influenced by fresh water discharge, which plays a key role in the variations of sea ice cover, its drift pattern, in maintaining the stratification of the Arctic Ocean and in influencing deep-water renewal in the Greenland Sea. In particular, the extent and thickness of sea ice cover influences the gas and energy balance between the atmosphere and the Arctic Ocean (Aagaard et al., 1985; Clark, 1990) and are thus affecting the global climate system.

Even if the importance of aerosol deposition (Shevchenko et al., 1995) and the biological productivity are considered, the most important Arctic sediment source is the input of river-derived suspended particulate matter (SPM). In this context, a unique phenomenon in the Siberian shelf seas is the incorporation of mostly fine-grained sediments into freshly formed sea ice, which is referred to as ice rafted sediments (IRS). Different processes for particle entrainment are discussed like scavenging of SPM from the water column due to frazil ice (cf. Reimnitz et al., 1992) or processes related to propagating wave fields into sea ice (cf. Ackermann et al., 1994). Studies of the sediment content of multi-year ice in the Transpolar Drift and the Eurasian Arctic suggest that a major fraction of the inorganic particulate load in the ice originates from the Siberian shelves and in particular from the Laptev Sea (Pfirman et al., 1990; Wollenburg, 1993; Nürnberg et al., 1994).

A natural geochemical pair of tracers to study the dispersion of river SPM throughout the Arctic Ocean is the Rb/Sr isotope system (Biscaye, 1971; Goldstein and Jacobsen, 1987, 1988; Palmer and Edmond, 1992; Douglas et al., 1995; Revel et al., 1996) because SPM is marked by unique $^{87}Rb/^{86}Sr$ and $^{87}Sr/^{86}Sr$ ratios. These ratios are primarily controlled by their Rb and Sr composition, geological origin and average mineral ages (^{87}Rb decays to ^{87}Sr with a half-life of $4.89 \pm 0.04 \times 10^{10}$ years; (Neumann and Huster, 1976; Davis et al., 1977). In fine-grained SPM (i.e., clays) minerals are common which tend to be enriched in Rb showing relatively high $^{87}Sr/^{86}Sr$ ratios (Goldstein and Jacobsen, 1987; Douglas et al., 1995). In contrast, in coarser grained SPM Sr is enriched relative to Rb showing relatively low $^{87}Sr/^{86}Sr$ ratios (Biscaye, 1971; Goldstein and Jacobsen, 1987; Douglas et al., 1995). Thus, individual river SPM samples may form Rb/Sr isochrons defined by two endmembers. One endmember are suites enriched in large grain sizes and the other endmember are suites enriched in small grain sizes. Given that the chemical alteration is negligible (i.e., closed system behaviour) the slope of the isochron then reflects the average age of the source rocks and the initial $^{87}Sr/^{86}Sr$ ratio the geological origin of the SPM (Biscaye, 1971).

In this study, we use the Rb/Sr isotope systematic of East Siberian river SPM, IRS, Arctic Ocean surface sediments and Laptev Sea sediments in order to constrain provenance and fluvial SPM dispersion throughout the Arctic Ocean.

2. Geology and hydrology of the Lena, Yana and Khatanga drainage basins

The geographical and geological characteristics of the Laptev Sea region and the Lena, Yana and Khatanga drainage areas summarised in Fig. 1 are based on a compilation in (Rachold et al., 1996). For further detailed information on the geology and hydrology of the Lena and Khatanga drainage areas we refer to the extensive studies of Huh et al. (1998a,b).

Six major rivers (Khatanga, Anabar, Olenjok, Lena, Omoloy and Yana) drain into the Laptev Sea (Fig. 1). The drainage areas of these rivers consist of six major geologic units which are labelled A to F in Fig. 1. The Siberian Platform (A) is composed mainly

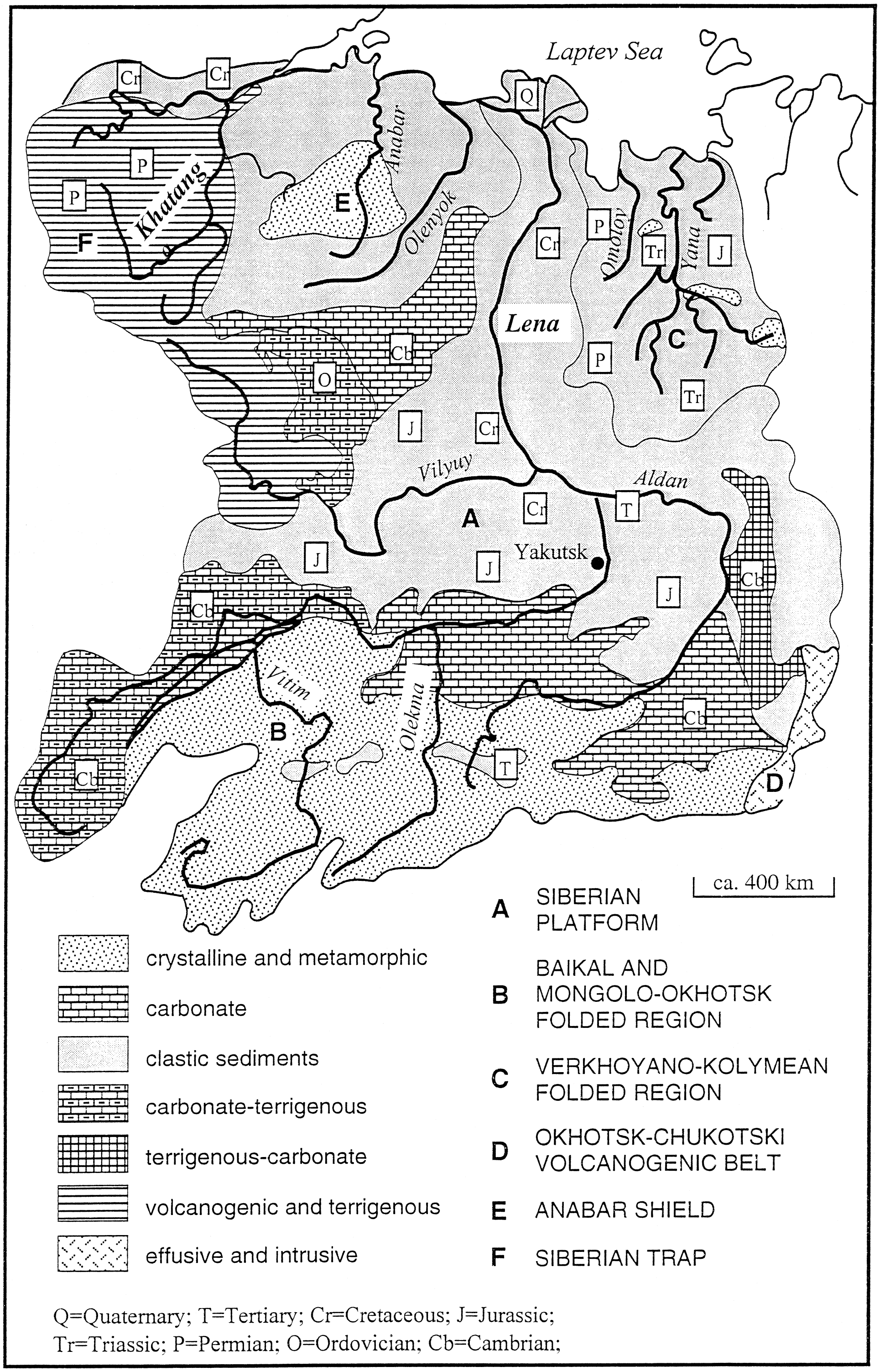

Fig. 1. Geologic units (A–F) of the Khatanga, Lena and Yana drainage area.

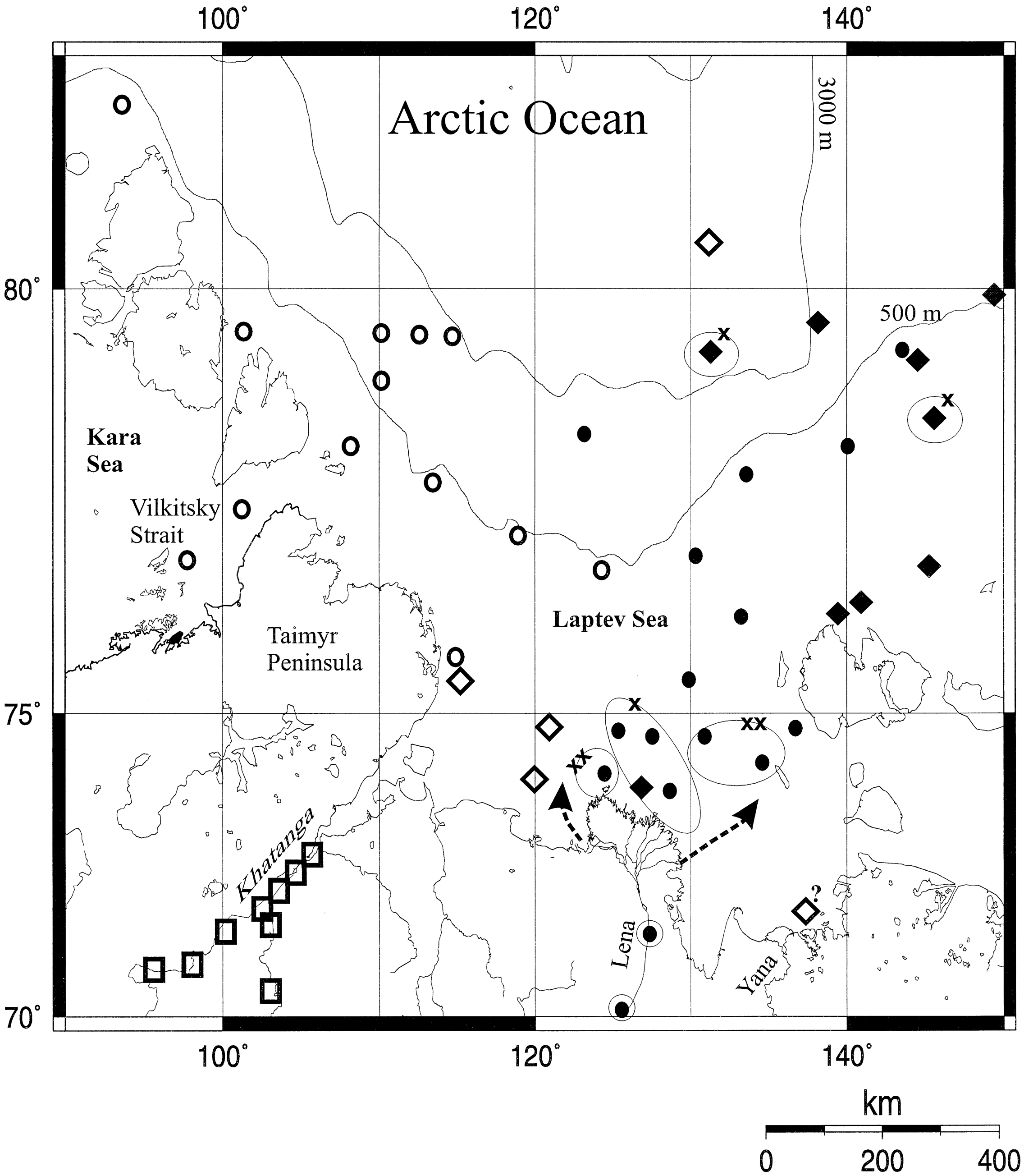

Fig. 2. Sample locations of the Laptev Sea area. Circles mark surface sediments and squares mark IRS samples. Filled black symbols mark sediments which are isotopically related to Lena derived SPM. Open symbols represent sediment samples which are isotopically a mixture of Lena SPM, Khatanga SPM and Kara Sea sediments. Samples marked with -×- represent sediments with the largest $^{87}Rb/^{86}Sr$ and $^{87}Sr/^{86}Sr$ ratios. Samples marked with -××- indicate sediments with lowest $^{87}Rb/^{86}Sr$ and $^{87}Sr/^{86}Sr$ ratios. Arrows mark major water outflows from the Lena delta. Note: the most drastic changes of the Rb/Sr systematics occur close to the Lena mouth.

of Cambrian and Precambrian limestone, terrigenous sediments of Jurassic to Cretaceous age and Quaternary alluvial deposits. Its north-western part is formed by volcanic rocks (F) of Permian age (Kamo et al., 1996). The south-eastern region (Aldan highland) is composed of Archean and Proterozoic crystalline and metamorphic rocks. The Baikal folded region (B) consists of gneisses, schist, quartzite and mar-

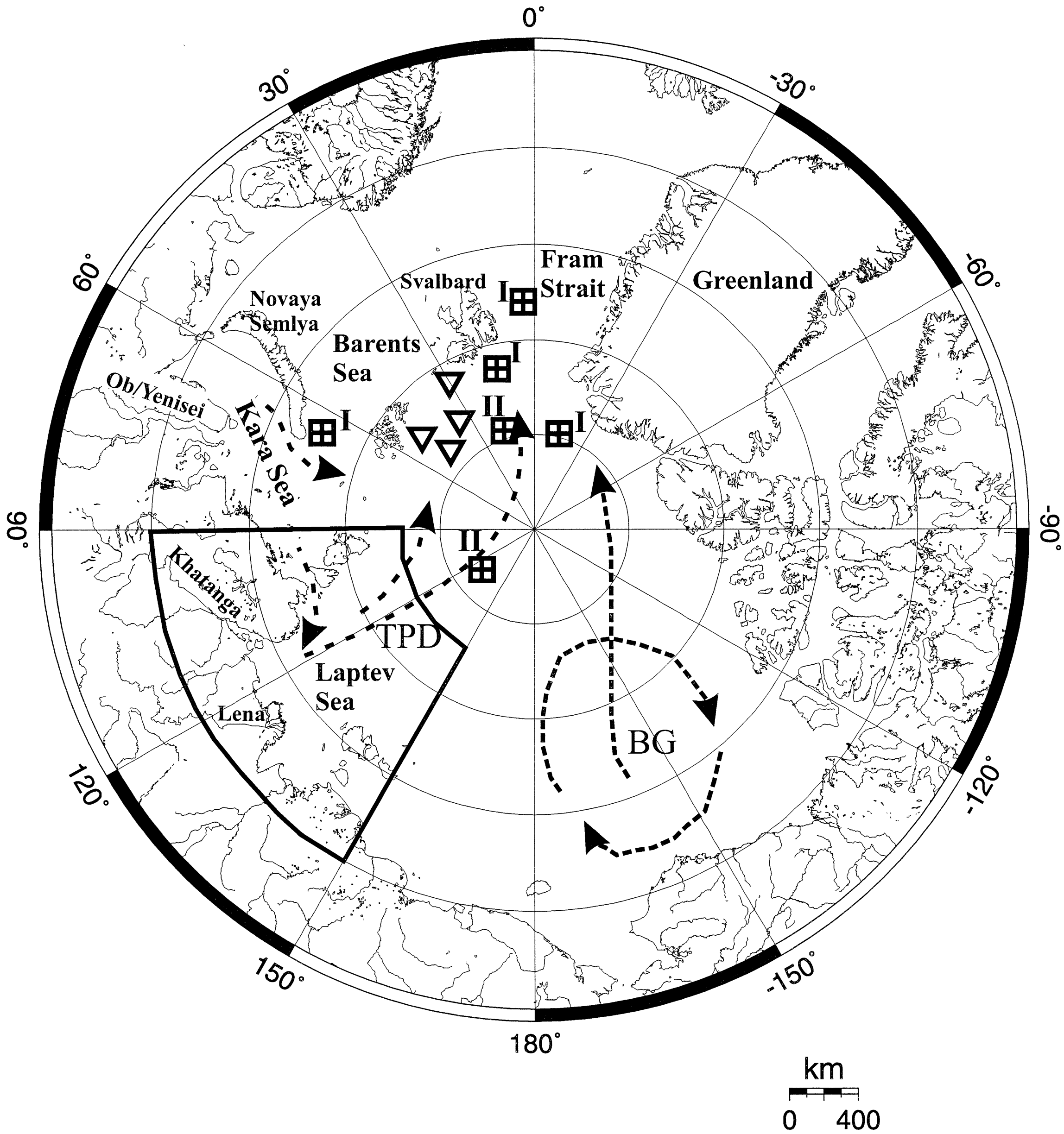

Fig. 3. Sample locations of the Arctic Ocean. Squares mark surface sediments and triangles mark IRS samples. Dotted lines mark the trajectory of major water outflow from the Laptev Sea and the Kara Sea. TPD: Transpolar Drift; BG: Beaufort Gyre. Samples marked with -II- originate from the Lena drainage area and/or the Siberian flood basalt. Sediments marked with -I- neither originate from the Lena drainage area nor from the Siberian flood basalt.

bleised limestone of Proterozoic age. In the Verkhoyano–Kolymean folded region (C) Permian and Carboniferous terrigenous sediments as well as volcanic rocks and granitoids of Triassic and Jurassic age are more common (Gordeev and Sidorov, 1993; Alabyan et al., 1995).

Sedimentological investigations show that the sand abundance on the western Laptev Sea shelf (west of about 120°E) is about a factor of two higher compared to the eastern Laptev Sea shelf (east of 120°E) (Wahsner, 1995). On the eastern Laptev Sea shelf the smectite abundance is about 5% to 20% of the total sediment, whereas on the western Laptev Sea shelf smectite is more abundant in the range of about 20% to more than 40%. The opposite is observed for illite. On the eastern Laptev Sea shelf illite varies between 40% and about 60% in the total sediment fraction and on the western Laptev Sea shelf between 25% and about 45% (Silverberg, 1972; Larssen et al., 1987).

Because smectite is commonly a weathering product of basic volcanogenic rocks (Heim, 1990; Köster, 1993) smectite abundance on the western Laptev Sea shelf has been attributed to the input of the Khatanga and Anabar river draining the Siberian flood basalt. However, sedimentation in the adjacent Kara Sea is controlled by the sediment supply of the Ob and Yenisei river system draining the same basalt complex as the Khatanga. Therefore, the relatively high abundance of smectite on the western Laptev Sea shelf may also be attributed in part to the import of Kara Sea sediments (Wahsner, 1995).

Water masses and SPM from the Kara Sea are entering the western Laptev Sea through the Vilkitsky Strait (Figs. 2 and 3). In the western Laptev Sea these waters mix with Khatanga- and in the eastern Laptev Sea with Lena/Yana-river water. Sea surface currents leave the eastern Laptev Sea towards the east into the East Siberian Sea and the north towards the open Arctic Ocean contributing water and SPM to the Transpolar Drift (Gorshkov, 1983).

3. Sample preparation and analytical methods

The SPM sampling is described in detail in (Rachold et al., 1996) and in (Rachold et al., 1998). For Nd-, Rb- and Sr-isotope measurements we extracted the < 63 μm grain size fraction. Although the analysed spit of the sample is only a fraction of the bulk sediment, the measured results represent the Rb and Sr concentration of the whole sample because the larger grain sizes are dominated by quartz, in which Sr and Rb concentrations are negligible. Note, in order to study the grain size dependence of the Sr isotopes we selected the silt and clay fraction rather than the clay fraction only. Focusing on the clay fraction alone would be problematic because there are many samples where the clay fraction is too small to perform this study.

The formation of authigenic phases (e.g., the formation of Fe/Mn-oxyhydroxide coatings) can influence the original isotopic composition of the particles. Andersson et al. (1994) showed that the co-precipitation of Sr with Mn and Fe greatly diminished the difference in Sr isotopic composition between dissolved and suspended load. This is demonstrated by the fact that $\Delta\varepsilon_{Sr}$ values are close to zero when the Fe/Al ratio greatly exceeds the average crustal Fe/Al ratio. In order to remove any authigenic phases (e.g., Mn/Fe-oxyhydroxide coatings) and to extract the original detrital Sr ratios and concentrations, the marine sediment samples are leached with 1.3 N HCl. In particular, marine calcium carbonate contains high concentrations of Sr whose isotopic composition is that of sea water ($^{87}Sr/^{86}Sr$: 0.709063; cf. Faure, 1986) and, thus, would superimpose variations in the detrital Sr-fraction (Biscaye, 1971). Verification of this leaching treatment does not show any measurable effect on the Sr concentration and ratios of the investigated terrigenous sediments which is in accordance with recent results of (Asahara et al., 1995).

All samples were spiked for ^{150}Nd, ^{149}Sm, ^{87}Rb and ^{84}Sr before digestion in a mixture of HF, $HClO_4$ and HNO_3. Rb, Sr and Nd are chromatographically separated and extracted using ion exchange columns and then loaded on outgassed Ta- and Re-filaments, respectively. Rb concentrations were measured with the single filament technique by isotope dilution on a Teledyn 1260 mass-spectrometer in peak jumping mode. Sr- and Nd-isotope ratios were measured with single and double filament techniques, respectively, on a Finnigan MAT 262 RPQ^{+} in static mode.

Blanks for Sr were determined at about 1 ng for Sr which results from the complex sample preparation. However, sample sizes are sufficiently large (ca. 3 μg of Sr) that blank corrections are negligible. The accuracy of our Sr measurements is estimated by 29 determinations of the NBS standard 987 which gave a mean $^{87}Sr/^{86}Sr$ ratio (2 standard deviations) of 0.710251(15). Blanks for Nd are estimated to be about 0.7 ng. The accuracy for the Nd measurements was determined from 10 measurements of the La Jolla standard which gave a mean $^{143}Nd/^{144}Nd$ ratio of 0.511850(10). Other geochemical data were determined by XRD following standard procedures.

4. Results

4.1. Nd-, Rb-, Sr-isotope concentrations and ratios

Results for Nd-, Rb- and Sr-concentrations and isotope ratios are given in Table 1 and are graphically displayed in Fig. 4. The Sr isotopic systematic of the Khatanga, Lena and Yana river SPM are extensively discussed by Rachold et al. (1998). The Rb concentrations measured for this study vary between 132 ppm and 41 ppm. The highest Sr concentration in the marine sediments was 298 ppm and the lowest was 93 ppm, both sampled close to the Lena mouth. $^{87}Rb/^{86}Sr$ ratios vary between 0.56 in a sample from the Khatanga river and 3.35 in an IRS sample. $^{87}Sr/^{86}Sr$ ratios of all samples vary between 0.72259 in the Arctic Ocean and 0.71218 in an IRS sample from the western Laptev Sea (Fig. 2). For selected samples, Nd-concentrations and $^{143}Nd/^{144}Nd$ ratios are available. Nd-concentrations vary in a narrow range between 18 ppm and 23 ppm and ε_{Nd} values vary between about -17 and -8 (for calculation see Table 1).

In Fig. 4, the scatter of the data forms arrays where samples with high $^{87}Rb/^{86}Sr$ tend to have high $^{87}Sr/^{86}Sr$ ratios. In order to demonstrate that there is a genetic link between river SPM and marine sediments, two envelopes are defined approximately following the slopes provided by the Lena SPM and Khatanga SPM (Fig. 4). The envelope defined by the Lena SPM is referred to as the ‘LME’ and the envelope defined by the Khatanga SPM is referred to as the ‘FBE’. Although there are four Arctic Ocean sediment samples which plot above the defined envelopes all other samples fall within or between them.

Comparison of geographical locations (Fig. 2) with the defined envelopes (Fig. 4) reveals that all shelf and IRS samples that fall along the LME are from the eastern Laptev Sea (roughly about east of 120°E; marked with filled black symbols in Figs. 2 and 3). All other shelf sediments except one, and IRS samples that plot between the LME and FBE, originate from the western Laptev Sea (marked with open symbols in Figs. 2 and 3).

There are two sediment samples from the Arctic Ocean (marked with -II- in Fig. 3) which fall between the LME and FBE. In addition, four IRS samples from the northern Barents Sea can be attributed to LME and FBE, respectively. Four Arctic Ocean sediment samples (marked with -II- in Fig. 3) located at the exit of the Kara Sea, the Fram Strait, close to Svalbard and Greenland plot distinctly above the defined envelope. These samples may not be related to the Lena SPM or material originating from the Siberian flood basalt province.

4.2. ‘Pseudo-isochrons’ due to grain size separation

The shelf sediments may be considered to be a mixture of fluvial material originating from the major rivers draining into the Laptev Sea. Following this approach we would expect the Sr isotope ratios of all shelf sediments to fall along a mixing line provided by the average isotopic compositions of the Lena and Khatanga river SPM. From Fig. 5 it can be seen that all averaged marine samples show higher $^{87}Rb/^{86}Sr$ ratios than the river SPM values. This distribution cannot be explained by simple binary sediment mixing between Lena and Khatanga SPM. Thus, the line with positive slope formed by the average Lena river SPM, eastern Laptev Sea sediments and IRS samples (Fig. 5) must be caused either by sediment mixing with a second not observed endmember or by sediment unmixing process. Sediment mixing can be excluded because careful examination of possible sources reveals that there is no suitable sediment endmember in the circum-Arctic area to account for it.

If sediment unmixing creates such an envelope, then Sr concentrations and isotope ratios of a given suite of particles must vary with grain size. In order

Table 1
Sr-measurements on Arctic river SPM and sediment surface samples

Lab. label	Sample location or sediment core	Location	River/ water depth (m)	Sr (ppm)	$^{87}Sr/^{86}Sr$	Rb (ppm)	$^{87}Rb/^{86}Sr$	Nd (ppm)	ε_{Nd}
5	PC 30; St. 16	66°41.1′N 123.29.5′E	Lena	245	0.71539(1)	95	1.12	–	–
6	PC 36; St. 19	68°15.1′N 123°57.8′E	Lena	235	0.71608(2)	92	1.13	–	–
7	PC 39; St. 20	70°51.5′N 127°33.1′E	Lena	222	0.71602(2)	101	1.31	–	–
8	PC 47, St. 24	72°29.0′N 126°40.0′E	Lena	197	0.71651(2)	104	1.52	–	–
10	PC 61; St. 35	71°18.1′N 135°59.8′E	Yana	153	0.71401(2)	77	1.45	–	–
11	PC 64; St. 38	70°45.5′N 136°04.0′E	Yana	153	0.71413(2)	77	1.45	–	–
12	PC 66; St. 39	70°13.4′N 135°06.9′E	Yana	151	0.71416(2)	82	1.57	–	–
13	PC 68; St. 40	69°43.1′N 135°04.4′E	Yana	149	0.71405(2)	84	1.63	–	–
14	PC 71; St. 42	68°36.4′N 134°39.6′E	Yana	163	0.71365(2)	86	1.52	–	–
15	PC 73; St. 44	67°32.9′N 134°01.9′E	Yana	142	0.71586(2)	89	1.81	–	–
16	PC 74; St. 45	67°27.3′N 133°13.1′E	Sartang	146	0.71530(2)	115	2.27	–	–
17	PC 75; St. 46	67°29.6′N 133°14.5′E	Dulgalak	137	0.71689(2)	74	1.56	–	–
18	PC 79; St. 50	68°44.6′N 134°20.4′E	Bytaktay	144	0.71502(2)	87	1.74	–	–
19	KHA-Sr-1	71°34.1′N 99°37.7′E	Khita	206	0.70861(1)	41	0.57	–	–
20	KHA-Sr-2	71°45.1′N 100°57.5′E	Khita	204	0.70876(1)	42	0.59	–	–
21	KHA-Sr-3	71°54.1′N 102°00.6′E	Khita	212	0.70930(1)	41	0.56	–	–
22	KHA-Sr-4	71°30.6′N 103°11.7′E	Kotuy	169	0.71015(1)	59	1.01	–	–
23	KHA-Sr-5	71°51.9′N 102°07.7′N	Kotuy	170	0.71021(1)	60	1.02	–	–
24	KHA-Sr-6	71°58.4′N 102°23.7′E	Khatanga	202	0.70926(1)	47	0.68	–	–
25	KHA-Sr-7	72°46.2′N 105°14.3′E	Khatanga	183	0.71040(1)	65	1.03	–	–
27	KHA-Sr-9	72°16.4′N 103°05.2′E	Khatanga	203	0.70925(1)	58	0.82	–	–
28	KHA-Sr-10	73°37.4′N 109°42.7′E	Khatanga	212	0.71217(1)	48	0.65	–	–
30	PM9417(0–1)	75°30.2′N 130°00.8′E	51	162	0.71736(1)	111	1.98	–	−13.5
31	PM9441(1–2)	74°00.0′N 125°59.4′E	14	290	0.71552(1)	81	0.81	–	−17.2
32	PM9442(1–4)	74°29.9′N 126°00.2′E	40	131	0.71844(1)	117	2.58	–	–
33	PM9451	74°30.2′N 130°29.7′E	25	298	0.71576(1)	80	0.77	–	–
34	PM9462(1–2)	74°30.1′N 136°00.2′E	27	152	0.71772(1)	114	2.16	–	–
35	PM9463(1–2)	74°30.2′N 126°34.9′E	36	133	0.71872(1)	113	2.45	–	–
36	PM9481(1–2)	73°45.0′N 134°00.3′E	17	270	0.71541(1)	77	0.82	–	–
37	PM9482(0–1)	73°59.9′N 128°10.5′E	27	120	0.72007(1)	119	2.86	–	−12.7
38	PM94T3(0–1)	77°04.2′N 99°13.2′E	110	132	0.71580(1)	103	2.25	–	−8
39	PM9402(0–1)	75°29.4′N 115°14.9′E	47	178	0.71434(1)	81	1.31	–	−10.6
40	PS2450-2	78°02.0′N 102°18.5′E	152	153	0.71536(1)	106	2	–	−8.6
41	PS2453-2	76°30.5′N 133°21.3′E	38	162	0.71798(1)	113	2.01	–	−12.1
42	PS2461-2	77°54.6′N 133°33.3′E	73	190	0.71623(1)	116	1.76	–	−11.4
43	PS2463-3	77°01.8′N 126°24.8′E	92	154	0.71584(1)	115	2.16	–	−11.1
44	PS2478-3	77°10.3′N 118°42.6′E	101	175	0.71398(1)	98	1.62	–	−9.7
45	PS2480-2	78°15.7′N 109°14.7′E	51	150	0.71517(1)	103	1.98	–	−7.9
46	PS2725-3	78°39.4′N 144°07.9′E	77	154	0.71680(1)	123	2.31	–	–
47	PS2726-5	77°59.7′N 140°05.4′E	48	179	0.71636(1)	107	1.73	–	–
48	PS2730	76°53.1′N 129°59.7′E	60	150	0.71827(1)	120	2.31	–	–
49	PS2745-7	80°24.9′N 102°05.4′E	255	133	0.71678(1)	92	2	–	–
50	PS2780-5	77°54.3′N 113°44.6′E	135	152	0.71403(1)	95	1.8	–	–
51	PS2789-5	81°57.5′N 91°06.0′E	235	128	0.71753(1)	112	2.53	–	–
52	KD95 2830160	76°03.1′N 139°35.3′E	–	164	0.71711(1)	117	2.1	–	–
53	KD95 2830460	76°09.5′N 139°02.6′E	–	197	0.71651(1)	93	1.36	–	–
54	KD95 2860160	71°38.0′N 135°22.1′E	–	93	0.71742(1)	108	3.35	–	–
55	KD95 2920160	70°40.4′N 126°51.5′E	–	133	0.71852(1)	110	2.39	–	–
56	KD95 2940160	73°50.5′N 120°18.0′E	–	152	0.71613(1)	98	1.86	–	–
57	KD95 2940460	73°57.0′N 121°46.0′E	–	167	0.71546(1)	97	1.68	–	–

Table 1 (continued)

Lab. label	Sample location or sediment core	Location	River/ water depth (m)	Sr (ppm)	$^{87}Sr/^{86}Sr$	Rb (ppm)	$^{87}Rb/^{86}Sr$	Nd (ppm)	ε_{Nd}
58	KD95 2950361	75°31.1′N 113°33.5′E	–	146	0.71515(1)	102	2.02	–	–
59	AR 1120561	76°31.5′N 145°44.1′E	–	195	0.71610(1)	91	1.35	–	–
60	AR 1120901	78°08.6′N 146°21.0′E	–	129	0.71926(1)	123	2.75	–	–
61	AR 1121013	78°39.2′N 144°07.1′E	–	150	0.71791(1)	129	2.48	–	–
62	AR 1122951	79°09.0′N 131°51.0′E	–	125	0.71865(1)	104	2.4	–	–
63	AR 1123252	80°54.0′N 131°0.2′E	–	166	0.71218(1)	58	1.01	–	–
64	AR 1124151	80°04.3′N 150°10.8′E	–	167	0.71768(1)	123	2.13	–	–
65	AR 1124205	78°2.66′N 135°00′E	–	154	0.71850(1)	110	2.06	–	–
67	PS1235 (0–10 cm)	78°51.6′N 1°18.6′E	2456	151	0.72003(1)	109	2.08	–	−12.7
68	PS2200 (5–10 cm)	85°19.4′N 14°00.0′E	1073	197	0.71911(1)	82	1.2	–	−11.6
69	PS1533-3	82°01.9′N 15°10.7′E	2030	149	0.72259(1)	108	2.1	–	–
70	PS2177-1	88°02.2′N 134°55.1′E	1388	197	0.71516(1)	132	1.93	–	−10.8
71	PS2195	86°13.7′N 09°35.6′E	3873	194	0.71605(1)	128	1.9	–	−11.2
72	PS464-2	77°28.8′N 125°54.2′E	2025	173	0.71683(1)	127	2.11	–	–
74	LO-94-58	77°33.7′N 71°59.2′E	308	142	0.71988(2)	100	2.03	–	–
75	Ark2401 (Kara Sea)	ca. 78°N 100°E	–	118	0.71531(1)	100	2.45	20.21	−8.9
76	Ark2512 (Laptev Sea)	ca. 79°N 115°E	–	183	0.71360(1)	83	1.31	21.95	−11.7
77	Ark2531 (Laptev Sea)	ca. 79°N 114°E	–	142	0.71394(1)	85	1.73	22.12	−9.1
78	Ark2581 (Laptev Sea)	ca. 79°N 110°E	–	129	0.71452(1)	97	2.17	21.82	−8.5
79	Ark2621 (Laptev Sea)	ca. 78°N 110°N	–	122	0.71463(1)	95	2.25	22.04	−9.3
80	Ark2241 (Cent. Arctic)	ca. 82°N 19°E	–	163	0.71313(1)	92	1.63	20.65	−8.4
81	Ark2281 (Cent. Arctic)	ca. 83.5°N 19.5°E	–	124	0.71489(1)	103	2.39	20.26	−9.5
82	Ark2291 (Cent. Arctic)	ca. 83.5°N 20.5°E	–	133	0.71489(1)	101	2.19	23.35	−8.7
83	Ark2331 (Cent. Arctic)	ca. 83.5°N 25°E	–	142	0.71399(1)	100	2.03	18.23	−8.5

Reported errors (in brackets) represent two standard deviations of the mean.
Statistical uncertainties for Sr- and Nd-concentrations are about 0.5%.
The ε_{Nd} values are calculated from $\varepsilon_{Nd} = [(^{143}Nd/^{144}Nd)_{Sample}/^{143}Nd/^{144}Nd)_{CHUR} - 1]10^4$; $(^{143}Nd/^{144}Nd)_{CHUR} = 0.512638$.

to test this hypothesis we measured the $^{87}Rb/^{86}Sr$ and $^{87}Sr/^{86}Sr$ ratios of two sediment samples (core 1533 from the Arctic Ocean; #69 in Table 1) as a function of their grain size. From Fig. 6A it can be seen that there is a positive relationship between the isotope ratios and the grain size distribution. A decrease of the grain size from about >20 μm to about 2 μm corresponds to an increase of the $^{87}Sr/^{86}Sr$ ratio from about 0.713 to more than about 0.730 and to an increase of the $^{87}Rb/^{86}Sr$ ratio from about 1 to about 6. This shows that Sr is enriched but less radiogenic in more coarse grained material. In more fine grained material, Sr contents are lower relative to Rb but tend to be more radiogenic. The spread of the $^{87}Rb/^{86}Sr$ and the $^{87}Sr/^{86}Sr$ ratios is larger than the spread of all sediment data. It is noteworthy that the grain size fractions of these two samples form parallel lines which can be regarded as 'pseudo-isochrons'. This verifies that individual Arctic ocean sediment samples keep their provenance information. In contrast, within the statistical uncertainties the $^{143}Nd/^{144}Nd$ ratios do not depend on their corresponding grain size distribution (Fig. 6B). These observations imply that variations of the Sr systematic in SPM are either due to grain size separation or to sediment mixing. However, concerning the Nd isotope systematic, variations can only be due to sediment mixing.

Here, we note that the FBE and LME arrays may also be considered as 'pseudo-isochrons' without representing any age of geological significance. This is because the Lena drainage area is geologically and geochronologically a heterogenous area. In this case the 'pseudo-isochron' is a mixing array formed by

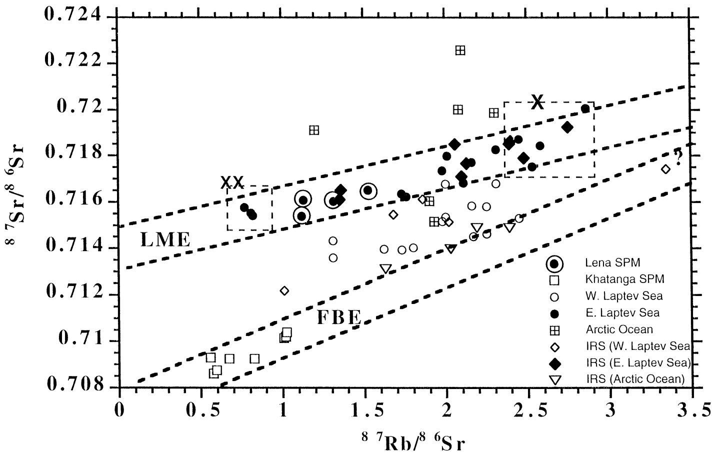

Fig. 4. $^{87}Sr/^{86}Sr$ ratios as a function of their corresponding $^{87}Rb/^{86}Sr$ ratios. Most data fall within or between two arbitrarily defined envelopes following the slopes provided by the Lena and Khatanga SPM. (LME: Lena Mixing Envelope; FBE: Flood Basalt Envelope). These envelopes or 'pseudo-isochrons' represent provenance and average age of the corresponding river drainage areas. Samples marked with -×- correspond to the finest grain size fraction (see also Fig. 2). Samples marked with -××- correspond to the coarsest grain size fraction.

relative contributions of weathering products of the youngest and oldest rock in this area. In addition, the minerals in an unmetamorphosed sedimentary rock would not define an isochron corresponding to the age of the sedimentary rock rather than the age of the original source rock, just as minerals from recent sediments in the Arctic Ocean do not define an isochron with age zero.

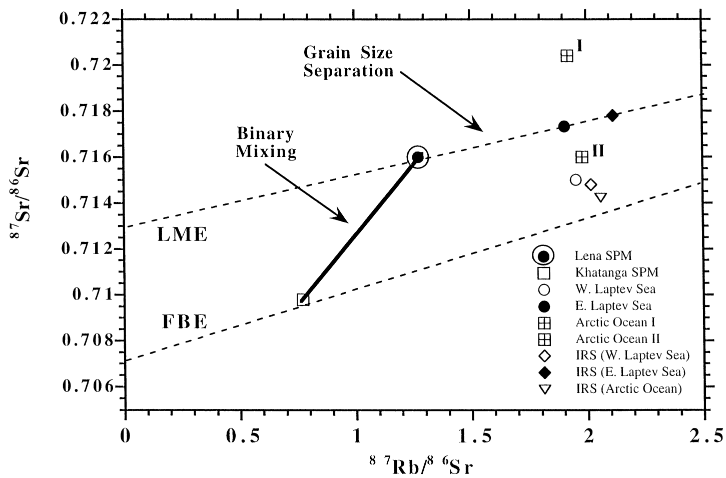

Fig. 5. Average $^{87}Sr/^{86}Sr$ ratios of river SPM and marine sediment samples are plotted as a function of their corresponding $^{87}Rb/^{86}Sr$ ratios. None of the average marine sediment samples plot along the binary mixing line provided by the Lena and Khatanga river SPM. However, eastern Laptev Sea sediments, IRS and Lena SPM form a line (LME) with positive slope which is interpreted to reflect grain size separation. Arctic Ocean sample marked by I represent the average value of those sediments plotting above LME and FBE. Arctic Ocean samples marked by II mark the average value of those sediments plotting in between LME and FBE.

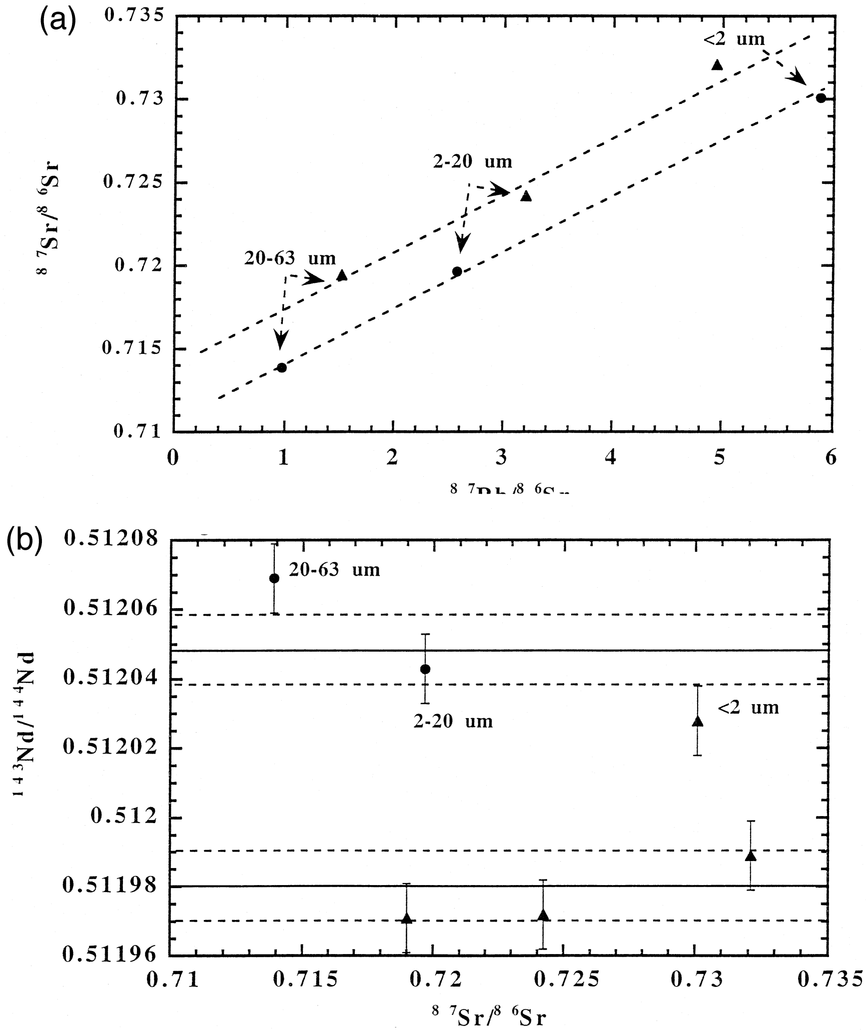

Fig. 6. (A) From two different Arctic Ocean bulk sediment samples marked by filled dots and triangles of sediment core 1533, it is experimentally verified that there is an inverse relationship between the $^{87}Rb/^{86}Sr$, the $^{87}Sr/^{86}Sr$ ratios and the particle grain size. The grain size derivatives form parallel trends with positive slopes which may be interpreted either as mixing lines or 'pseudo-isochrons' reflecting a mean age and provenance. (B) Within the accuracy of the external reproducibility (dotted lines) of the isotope measurement the $^{143}Nd/^{144}Nd$ ratio is independent from the grain size distribution.

4.3. Chemical weathering and closed system behaviour

It has been argued that there is almost no effect of chemical weathering on silicate rocks in the Lena drainage area because the Al and Fe elemental ratio of Lena river SPM compared to their source rock is close to 1 (Gordeev and Shevchenko, 1995). In order to further verify these earlier findings we calculated the index of chemical alteration for the Lena SPM (Chemical Index of Alteration $(CIA) = [Al_2O_3/(Al_2O_3 + CaO^* + Na_2O + K_2O)]$; McLennan, 1993). The CIA is a direct measure of the chemical alteration because feldspar and volcanic glass comprise some 75% of the labile weatherable material in the upper crust. Accordingly, much of the chemical variation resulting from weathering may be expressed in the system Al_2O_3–(CaO^*–Na_2O)–K_2O where CaO^* represents the Ca in the silicate fraction only. CIA values of about 45–55 indicate virtually no weathering (the average upper crust has a CIA value of about 47), whereas values of about 100 indicate intense chemical weathering with complete removal of the alkali and alkaline earth elements (McLennan, 1993). The calculated CIA of Lena river SPM is 45, which is very close to the average value of the upper crust. This low CIA value indicates that chemical weathering of silicates is negligible for the Lena drainage area and that the chemical composition of the river SPM is close to the original one of their source rocks. This implies that the samples falling along LME and FBE followed closed system behaviour for Rb/Sr.

However, it is noteworthy that numerous authors report that the first and most important silicate weathering reaction in periglacial environments is loss of interlayer K (and Rb) from biotite. This reaction could have a significant effect on Rb–Sr systematic without affecting the CIA measurably (Drever and Hurcomb, 1986; Blum and Erel, 1995; Anderson et al., 1997). Therefore, the CIA value may only be a necessity but not a sufficient criteria in order to verify closed system behaviour.

5. Discussion

5.1. Natural $^{87}Sr/^{86}Sr$ ratios and sediment unmixing in river SPM and marine sediments

When river SPM is delivered to the ocean and becomes marine sediment it faces a change in the chemical and physical environment at the transition from land to ocean. The original SPM grain size distribution and, hence, its isotope distribution may be rearranged due to a reduction of the transport velocity and to particle flocculation processes (Sholkovitz, 1976). Reduction of the particle transport velocity at the coastal zone causes preferential deposition of more coarse-grained material whereas the contact of river water with saline sea waters cause flocculation and deposition of fine grained particles (Sholkovitz, 1976). As a consequence of these processes the grain size distribution and the Rb/Sr isotope abundance of the marine sediments can be expected to differ from those of the river SPM. However, in the absence of chemical alteration the original provenance signal is still preserved in the Rb/Sr-isotope systematic because any variation of grain size distribution will change the $^{87}Sr/^{86}Sr$ ratios only along the slope of the original envelope. Given that chemical alteration is negligible, the LME and FBE reflect an apparent age and the geological origin of the corresponding drainage areas (LME: $^{87}Sr/^{86}Sr = 0.0017(^{87}Rb/^{86}Sr) + 0.714(1)$; FBE: $^{87}Sr/^{86}Sr = 0.00131(^{87}Rb/^{86}Sr) + 0.707(1)$). Calculations reveal apparent ages of about 120 Ma for the Lena drainage area (LME) and of about 220 Ma for the Siberian flood basalt province (FBE). The LME age is in general agreement with the depositional age of the Cretaceous and Jurassic sediments which are drained by the Lena river (Fig. 1) although we do not consider this age to be of any geological significance. This is because the Lena drainage area shows a large geological and geochronological heterogeneity and thus, the calculated apparent age may just accidentally reflect the depositional age of these sediments. Note, the extrapolated initial $^{87}Sr/^{86}Sr$ ratio of the Lena SPM of 0.713(1) points to crustal rocks as a source of the eroded material.

The age of 220 Ma calculated from the FBE is close to the age of about 250 Ma established from U/Pb dating of the Siberian flood basalt (Kamo et al., 1996). The initial $^{87}Sr/^{86}Sr$ of 0.707(1) extrapolated from the FBE is close to 0.704 which is supposed to be the initial $^{87}Sr/^{86}Sr$ ratio of mantle derived material being the source of the flood basalt (Faure and Powell, 1972).

The model presented above predicts the most drastic changes to occur close to the river mouth because of a reduction of the particle transport velocity and due to particle flocculation processes. In Fig. 2 three sediment samples are marked with (-××-) showing the lowest $^{87}Rb/^{86}Sr$ and $^{87}Sr/^{86}Sr$ ratios of all measured samples. Apparently, in these areas reduction of particle transport velocities caused a preferential deposition of coarse grained material. In addition, three sediment samples and one IRS sample are marked with (-×-) showing the largest $^{87}Rb/^{86}Sr$ and ratios of all samples (Fig. 2). In these areas more fine than coarse grained material is deposited because the process of particle flocculation dominates the process of velocity reduction.

The observed spatial distribution of the isotope ratios and, hence, grain size distribution reflect the outflow system of the Lena river, which is largest through the western and eastern river arms in the delta. The higher transport velocities of these main channels favour the deposition of more coarse-grained material into the adjacent Laptev Sea area. In contrast, in the central Lena delta the river water disseminates into second order river arms and transverse distributaries, which is accompanied by a general reduction of river water transport velocities (Alabyan et al., 1995). This favours the deposition of more fine-grained material in the Laptev Sea adjacent to the central Lena delta. There are two IRS samples which also show the highest $^{87}Rb/^{86}Sr$ and $^{87}Sr/^{86}Sr$ ratios. According to our model, these sediments must originate from the area in front of the central Lena delta, where the finest material is released into the Laptev Sea. This material is then incorporated into the sea ice either by suspension freezing directly from the water column or by sediment uptake from the sea floor. After incorporation this IRS is then drifted away to the position where it was sampled. Although it is not possible to make any more detailed inferences about the path of sediment incorporation into the sea ice the provenance can be identified from the Rb/Sr isotope systematic.

The Nd isotope systematic in the sediments have been proven to be independent of the grain size distribution (Fig. 6B), thus allowing a rough estimate of the relative sediment contribution to the Laptev Sea from the two endmembers. In Fig. 7, the Siberian flood basalt endmember (FBE) is marked with a mean ε_{Nd} value of 0 and by a $^{87}Sr/^{86}Sr$ ratio of about 0.705 (Sharma et al., 1992). The eastern Laptev Sea endmember (LME) is marked with mean ε_{Nd} and $^{87}Sr/^{86}Sr$ values of about -12.5 and 0.717, respectively. From Fig. 7, it can be seen that western Laptev Sea sediments (mean ε_{Nd}: -8.65, mean $^{87}Sr/^{86}Sr$: 0.715) fall along a mixing envelope between the Siberian flood basalt and the eastern Laptev Sea. From the given values it can be calculated that about 70% of the western Laptev Sea sediments are Lena SPM derivatives and that about 30% originate from the Siberian flood basalt.

However, the Khatanga contributes only about 7% of the Laptev Sea sediments (Gordeev et al., 1996) and can therefore not solely be responsible for the import of volcanogenic material to the western Laptev Sea. A second source could be the Ob/Yenisei river system which supplies the adjacent Kara Sea with volcanogenic weathering products (e.g., smectite) also originating from the Siberian flood basalt. A part of this supply may enter the western Laptev Sea through the Vilkitsky Strait (Figs. 2 and 3) which is also supported by independent mineralogical studies (Wahsner, 1995). Unfortunately, this predicted sediment import is difficult to quantify because Kara Sea sediments and Khatanga SPM originate from the same source and are isotopically indistinguishable. This is indicated by the fact that there are several samples from the Vilkitsky Strait and the Kara Sea plotting in between the LME and FBE (Figs. 2 and 4).

The surface sediments of the two central Arctic Ocean locations (marked with -I- in Fig. 3) originate from the Lena drainage area and the Siberian flood basalt province. This is indicated by the fact that their isotope ratios fall between LME and FBE (Figs. 4 and 7). Similar observation account for four Arctic IRS samples from the northern Barents Sea (Fig. 3).

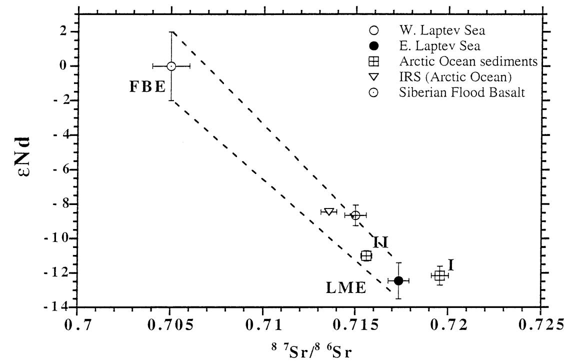

Fig. 7. Here, available ε_{Nd} values are plotted as a function of their corresponding $^{87}Sr/^{86}Sr$ ratios. Average isotope values of the eastern Laptev Sea corresponding to the LME and average isotope values (adopted from Sharma et al., 1992) from the Siberian flood basalt province (FBE) form two endmembers of a mixing envelope. Almost all investigated samples plot within the provided envelope. This may be interpreted that these sediments are a mixture of contributions from the Siberian flood basalt and to a larger extend from sediments of crustal origin supplied from the Lena drainage area. Arctic Ocean samples marked with -II- are neither related to the Lena drainage area nor to the Siberian flood basalt province.

These samples plot closest to the FBE envelope (Fig. 4) and show the highest ε_{Nd} value (-8.45) of all samples (Fig. 7) indicating that they are closest related to the Siberian flood basalt province. These findings support the inferences that sediments from the Kara Sea and the Laptev Sea are transported via the Transpolar Drift to the central Arctic Ocean, the Barents Sea and the Fram Strait.

All other sediment samples which are located at the Arctic Ocean margins (marked with -II- in Fig. 3) are isotopically related to neither the Lena drainage area nor to the Siberian flood basalt province, because their isotope ratios are distinctively incompatible with the defined envelopes (Figs. 4 and 7). It can be speculated that these sediments may reflect the influence of local sediment sources such as the Devonian rocks of the Hekla–Hoek-Formation on Svalbard (Birkenmajer, 1981). In addition, it seems possible that these sediments are influenced by sediments from the American Arctic which are transported via the Beaufort Gyre to the sea around Svalbard and to the Fram Strait. Rocks from Svalbard and from American Arctic terranes are both older than those of the Lena drainage area and the Siberian flood basalt, which would be in general accord with the more radiogenic $^{87}Sr/^{86}Sr$ ratios of these marked Arctic Ocean sediments.

6. Summary

(1) The Rb/Sr-isotope systematic have been performed on marine sediments and to SPM of major Siberian rivers (Lena and Khatanga) draining into the Laptev Sea. The distribution of the Sr in the marine environment is controlled by grain size separation processes such as the precipitation of large particles due to reduction of transport velocities at the transition from land to ocean and the flocculation of small grain size particle due to the contact with saline sea water.

(2) Because of negligible chemical weathering, the Rb/Sr isotope systematic follow closed system behaviour which reflect the average geochronological age of the drainage area and the initial isotope ratio the geological origin.

(3) The origin of marine sediments can be identified by comparison to the LME and FBE. All sediment data, except one sample, from the eastern part of the Laptev Sea fall along the LME. Almost all samples from the western part of the Laptev Sea, the northern Barents Sea and the central Arctic Ocean plot between the LME and the FBE.

(4) Mixing calculations reveal that about 70% of the western Laptev Sea sediments originate from the Lena drainage area and that about 30% are weathering products originating from the Siberian flood basalt. This material is delivered by the Khatanga and by the Ob/Yenisei river system via the Kara Sea and the Vilkitsky Strait into the western Laptev Sea. Relative contributions of Khatanga and Ob/Yenisei SPM are difficult to quantify because they are isotopically indistinguishable.

Acknowledgements

This study is supported by the 'Deutsche Forschungsgemeinschaft, Ei272/5-1' and by 'Verbundvorhaben System Laptev See' funded by the 'Bundesministerium für Bildung und Forschung'. The valuable comments of Prof. J. Hoefs, Prof. G. Wörner and Dr. B. Bock helped to improve this manuscript. H. Herborg, G. Mengel, K. Laschtowitz, L. Reese, E. Schiffczyk and R. Skrandies are gratefully acknowledged for laboratory help and computer assistance. Dr. A. Mickein is gratefully acknowledged for general support and discussions. Dr. C. Strobl (Heidelberg, Germany) and Dr. G.I. Ivanov (St. Petersburg, Russia) provided sample material. *[JD]*

References

Aagaard, K., Swift, J.H., Carmack, E.C., 1985. Thermohaline circulation in the Arctic mediterranean seas. J. Geophys. Res. 90, 4833–4846.

Ackermann, N.L., Shen, H.T., Sanders, B., 1994. Experimental studies of sediment enrichment of arctic ice covers due to wave action and frazil entrainment. J. Geophys. Res. 99 (C4), 7761–7770.

Alabyan, A.M., Chalov, R.S., Korotaev, V.N., Sidorchuk, A.Y., Zaitsev, A.A., 1995. Natural and technogenic water and sediment supply to the Laptev Sea. Rep. Polar Res. 176, 265–271.

Anderson, S.P., Drever, J.I., Humphrey, N.F., 1997. Chemical weathering in glacial environments. Geology 25, 399–402.

Andersson, P.S., Wasserburg, G.J., Ingri, J., Stordal, M.C., 1994.

Strontium dissolved and particulate loads in fresh and brackish waters: the Baltic sea and Mississippi Delta. Earth Planet. Sci. Lett. 124, 195–210.

Asahara, Y., Tanaka, T., Kamioka, H., Nishimura, A., 1995. Asian continental nature of $^{87}Sr/^{86}Sr$ ratios in north central Pacific sediments. Earth Planet. Sci. Lett. 133, 105–116.

Birkenmajer, 1981.

Biscaye, P.E., 1971. The rubidium, strontium, strontium-isotope system in deep-sea sediments: Argentine basin. J. Geophys. Res. 76 (21), 5087–5095.

Blum, J.D., Erel, Y., 1995. A silicate weathering mechanism linking increases in marine $^{87}Sr/^{86}Sr$ with global glaciation. Nature 373, 415–418.

Clark, D.L., 1990. Arctic Ocean ice cover; geologic history and climatic significance. In: Grantz, A., Johnson, L., Sweeney, J.F. (Eds.), The Arctic Ocean Region. Geol. Soc. Am., Boulder, CO, 53–62.

Davis, D.W., Gray, J., Cumming, G.L., Baadsgaard, H., 1977. Determination of the ^{87}Rb decay constant. Geochim. Cosmochim. Acta 41, 1745–1749.

Douglas, G.B., Gray, C.M., Hart, B.T., Beckett, R., 1995. A strontium isotopic investigation of the origin of suspended particulate matter (SPM) in the Murray–Darling River system, Australia. Geochim. Cosmochim. Acta 59 (18), 3799–3815.

Drever, J.I., Hurcomb, D.R., 1986. Neutralization of atmospheric acidity by chemical weathering in an alpine drainage basin in the North Cascade mountains. Geology 14, 221–224.

Faure, G., 1986. Principles of Isotope Geology. Wiley, New York, 1–589.

Faure, G., Powell, J.L., 1972. Strontium Isotope Geology. Springer-Verlag, Berlin, 1–188.

Goldstein, S.J., Jacobsen, S.B., 1987. The Nd and Sr isotopic systematics of river-water dissolved material: implications for the sources of Nd and Sr in seawater. Chem. Geol. 66, 245–272.

Goldstein, S.J., Jacobsen, S.B., 1988. Nd and Sr isotopic systematics of river water suspended material: implications for crustal evolution. Earth Planet. Sci. Lett. 87, 249–265.

Gordeev, V.V., Sidorov, I.S., 1993. Concentrations of major elements and their outflow into the Laptev Sea by the Lena River. Mar. Chem. 43, 33–45.

Gordeev, V.V., Shevchenko, V.P., 1995. Chemical composition of suspended sediments in the Lena river and its mixing zone. Rep. Polar Res. 176, 154–169.

Gordeev, V.V., Martin, J.M., Sidorov, I.S., Sidorova, M.V., 1996. A reassessment of the Eurasian river input of water, sediment, major elements, and nutrients to the Arctic ocean. American Journal of Science 296, 664–691.

Gorshkov, V.V., 1983. World Ocean Atlas—Arctic Ocean. 3, 1-80-103.

Heim, D., 1990. Tone und Tonminerale. Stuttgart, Germany (Enke).

Hölemann, J., Kassens, H., Schirmacher, M., Prange, A., 1996. Geochemistry of the Surface Sediments of an Arctic Shelf Sea: Laptev Sea, Siberia. EOS, Transactions, AGU 77/46, 377.

Huh, Y., Edmond, J.M., 1996. The isotopic systematics of fluvial Sr: New results from the big rivers of Eastern Siberia. EOS, Transactions, AGU 1996 Fall Meeting 77/46, 325.

Huh, Y., Chan, L.-H., Zhang, L., Edmond, J.M., 1998a. Lithium and its isotopes in major world rivers: implications for weathering and the oceanic budget. Geochim. Cosmochim. Acta 62 (12), 2039–2051.

Huh, Y., Tsoi, M.-Y., Zaitsev, A., Edmond, J.M., 1998b. The fluvial geochemistry of the rivers of Eastern Siberia: I. Tributaries of the Lena river draining the sedimentary platform of the Siberian Craton. Geochim. Cosmochim. Acta 62 (10), 1657–1675.

Kamo, S.L., Czamanske, G.K., Krogh, T.E., 1996. A minimum U–Pb age for Siberian flood-basalt volcanism. Geochim. Cosmochim. Acta 60 (18), 3505–3511.

Kassens, H., Bauch, H., Hölemann, J.A., Thiede, J., 1996. Holocene climatic changes in the Siberian Arctic: Implications from the Laptev sea shelf. EOS, Transactions, AGU 77/46, 413.

Köster, H.M., 1993. Beschreibung einzelner Tone. In: Jasmund, K., Lagaly, G. (Eds.), Tonminerale und Tone. Steinkopf Verlag, Darmstadt, 33–67.

Larssen, B.B., Elverhøi, A., Aagaard, P., 1987. Study of particulate material in sea ice in the Fram strait—a contribution to paleoclimatic research?. Rep. Polar Res. 5 (3), 313–315.

McLennan, S.M., 1993. Weathering and global denudation. The Journal of Geology 101, 295–303.

Neumann, W., Huster, E., 1976. Discussion of the ^{87}Rb half-life by absolute counting. Earth Planet. Sci. Lett. 33, 277–288.

Nürnberg, D., Dethleff, I.W., Eicken, D., Kassens, H. et al., 1994. Sediments in Arctic sea ice—implications for entrainment, transport and release. Mar. Geol. 119, 185–214.

Palmer, M.R., Edmond, J.M., 1992. Controls over the strontium isotope composition of river water. Geochim. Cosmochim. Acta 56, 2099–2111.

Pfirman, S., Lange, M.A., Wollenburg, I., Schlosser, P., 1990. Sea ice characteristics and the role of sediment inclusions in deep-sea deposition. In: Bleil, U., Thiede, J. (Eds.), Geological History of the Polar Oceans: Arctic versus Antarctic. Kluwer Academic Publishers, Dordrecht, 187–211.

Rachold, V., Alabyan, A., Huberten, H.W., Korotaev, V.N., Zaitsev, A.A., 1996. Sediment transport to the Laptev Sea—hydrology and geochemistry of the Lena river. Rep. Polar Res. 15, 183–196.

Rachold, V., Eisenhauer, A., Hubberten, H.-W., Hansen, B., Meyer, H., 1998. Sr isotopic composition of suspended particulate material (SPM) of East Siberian rivers—sediment transport to the Arctic ocean. Arctic and Polar Research 29 (4), 422–429.

Reimnitz, E., Marincovich, L., McCormick, M., Briggs, W.M., 1992. Suspension freezing of bottom sediment and biota in the Northwest Passage and implications for Arctic ocean sedimentation. Can. J. Earth Sci. 29, 693–703.

Revel, M., Sinko, J.A., Grousset, F.E., Biscaye, P.E., 1996. Sr and Nd isotopes as tracers of North Atlantic lithic particles: paleoclimatic implications. Paleoceanography 11, 95–113.

Sharma, M., Basu, A.R., Nesterenko, G.V., 1992. Temporal Sr-, Nd- and Pb-isotopic variations in the Siberian flood basalts:

implications for the plume source characteristics. Earth Planet. Sci. Lett. 113, 365–381.

Shevchenko, V.P., Lisitzin, A.P., Kuptzov, V.M., Ivanov, G.I., Lukasin, V.N. et al., 1995. The composition of Aerosols over the Laptev, the Kara, the Barents, the Greenland and the Norwegian sea. Rep. Polar Res. 176, 7–16.

Sholkovitz, E.R., 1976. Flocculation of dissolved organic and inorganic matter during the mixing of river water and seawater. Geochim. Cosmochim. Acta 40, 831–846.

Silverberg, N., 1972. Sedimentology of the Surface Sediments of East Siberian and Laptev Seas. PhD, Univ. of Washington.

Wahsner, M., 1995. Mineralogical and sedimentological characterization of surface sediments from the Laptev sea. Rep. Polar Res. 176, 303–313.

Wollenburg, I., 1993. Sedimenttransport durch das arktische Meereis: die rezente lithogene und biogene Mineralfracht. Rep. Polar Res. 127, 159.